

Econometrics as Sorcery

G. Innocenti and D. Materassi

Dipartimento di Sistemi e Informatica
 Centro per lo Studio di Dinamiche Complesse - CSDC
 Università di Firenze,
 via di S. Marta 3, 50139 Firenze, Italy
 tel: +39 055 4796 360.

Abstract. The paper deals with the problem of identifying the internal dependencies and similarities among a large number of random processes. Linear models are considered to describe the relations among the time series and the energy associated to the corresponding modeling error is the criterion adopted to quantify their similarities. Such an approach is interpreted in terms of graph theory suggesting a natural way to group processes together when one provides the best model to explain the other. Moreover, the clustering technique introduced in this paper will turn out to be the dynamical generalization of other multivariate procedures described in literature.

1. Introduction

Deriving information from data is a crucial problem in science and it has been widely investigated in literature. A large variety of contributions has been developed in many fields, such as engineering, physics, biology and economy, providing several methods and procedures which accomplish to different objectives [1, 2, 3, 4]. In particular, in the study of complex systems, the comprehension of the internal connections, which define the hierarchical structure of the process, turns out to play a key role to fully understand its dynamics. This is especially true in presence of a multivariate data set, because this kind of samples is usually the result of a process intrinsically organized into interconnected subsystems [5]. Therefore, the recognition of the system structure is a critical step for the definition of a suitable model. In particular, a clusterization problem can be solved to divide the source data set into interconnected homogeneous groups describing different subsystems [6]. This approach deals with the search of similarities and relations inside the original samples, trying to catch their internal connections and providing a schematic representation of hierarchies. Recently, new clustering techniques based on a correlation matrix have been proposed for the analysis of data sets made up by a large variety of time series [7, 8]. However, these procedures are able to detect only the “static” relations among the samples, since they capture the similarities just at the current time [9, 10, 11].

In this paper, we propose a clustering technique based on a modeling approach. Indeed, since the original time series are dynamically interconnected, we intend to derive their hierarchy in terms of mathematical laws, which provide a structured description of the internal mechanics. To this aim, we settle the clustering problem into the framework of the system identification theory [12, 13]. Hence, exploiting the modeling errors to quantify the similarities among the original signals, we realize a

clustering technique, defined as the solution of a minimization problem. Therefore, a modeling interpretation of the procedures based on the correlation matrix is first introduced. In particular, they turn out to be a non optimal choice with respect to the modeling error. Then, the approach is developed taking into account dynamic dependencies among the time series. To this regard, the identification step is realized introducing the hypothesis of linear dynamic connections, represented by Single Input-Single Output (SISO) local models. Moreover, since the clusters are internally organized by means of transfer functions, the final model can be interpreted as a dynamical network of interconnected systems and its structure as the related topology.

Notation:

$E[\cdot]$: mean operator;

$R_{XY}(\tau) \doteq E[X(t)Y(t+\tau)]$: cross-covariance function of stationary processes;

$R_X(\tau) \doteq R_{XX}(\tau)$: autocovariance;

$\rho_{XY} \doteq \frac{R_{XY}}{\sqrt{R_X R_Y}}$: correlation index;

$\mathcal{Z}(\cdot)$: Zeta-transform of a signal;

$\Phi_{XY}(z) \doteq \mathcal{Z}(R_{XY}(\tau))$: cross-power spectral density;

$\Phi_X(z) \doteq \Phi_{XX}(z)$: power spectral density;

with abuse of notation, $\Phi_X(\omega) = \Phi_X(e^{i\omega})$;

$\lceil \cdot \rceil$ and $\lfloor \cdot \rfloor$: ceiling and floor function respectively;

$(\cdot)^*$: complex conjugate.

2. A Modeling Perspective

In [9] a procedure to obtain a hierarchical structure of a set of time series is proposed. N realizations of N random processes X_i are considered. First, an estimation of the correlation index ρ_{ij} related to every couple (X_i, X_j) is computed, along with the associated distances (see [4])

$$d_{ij} \doteq \sqrt{2(1 - \rho_{ij})} . \quad (1)$$

Then, a graph is defined where every node represents a random process and the arc linking two nodes is weighed according to (1). Eventually, the Minimum Spanning Tree (MST) is extracted by the graph. This procedure has been successfully exploited to provide a quantitative and topological analysis of time series, especially in the economic field (see [4], [8] and [11]). It is worth considering that such a technique can be interpreted in terms of a modeling procedure. Consider the problem of describing a process X_j by scaling another process X_i with a suitable real constant α_{ji} . Choosing

$$\alpha_{ji} = \sqrt{\frac{E[X_j^2]}{E[X_i^2]}} = \sqrt{\frac{R_{X_j}}{R_{X_i}}} , \quad (2)$$

we find that

$$E[(X_j - \alpha_{ji}X_i)^2] = E[X_j^2] d_{ij}^2.$$

Hence, the distance (1) can be interpreted as the root of the mean square error, properly normalized by the variance of X_j , when the simple gain (2) is used. Such a normalization is necessary since we are interested into capturing similar trends between

the processes regardless of their amplitudes. However, we remark that the choice of (2) can be considered arbitrary. Conversely, we would like to evaluate the closeness of two processes according to the information which can be inferred about one of them assuming to know the other [14]. From this point of view, (2) does not satisfy any optimality criterion. Indeed, considering two anticorrelated time series ($\rho_{ij} = -1$) it is possible to perfectly reconstruct one from the other. Thus the information in the two signals is the same, while their distance (1) makes them the farthest away.

Let us define

$$e_{ji} = X_j - \alpha_{ji}X_i, \quad (3)$$

then, it is possible to adopt the least squares criterion in order to evaluate the “best” constant α_{ji} . In this case, it is immediate to prove that the optimal choice is given by

$$\hat{\alpha}_{ji} = \frac{R_{X_j X_i}}{R_{X_i}} \quad (4)$$

and the relative quadratic error amounts to

$$E[e_{ji}^2] = R_{X_j} - \frac{R_{X_j X_i}^2}{R_{X_i}} \quad (5)$$

(see [13]). In order to obtain an adimensional quantity, we can normalize (5) with respect to the power of X_j and define the binary function

$$d(X_i, X_j) \doteq \sqrt{\frac{E[e_{ji}^2]}{R_{X_j}}} = \sqrt{1 - \rho_{X_i X_j}^2}. \quad (6)$$

It is worth observing that (6) is a distance exactly as (1).

Proposition 1. *The function $d(\cdot, \cdot)$, as defined in (6), is a metric.*

Proof. See the appendix. \square

In [9], the MST is extracted from the graph, according to the weights (1). This is equivalent to define a hierarchical structure of the time series relying on the adoption of linear gain models (2) between the processes and considering the relative modeling error as a distance function.

Substituting (1) with (6), we are applying the same topological strategy, but we are structuring the data according to the the best gain model in the sense of the least squares.

Remark 2. *From a system theory point of view, it can be said that both the approaches are “static”. Indeed, the models do not have a state, thus they do not have any dynamics. They simply capture a direct relation between two process samples at the same time instant. However, the optimal approach we have followed can be extended to a more general case.*

3. Dynamic Modeling using Wiener Filters

We consider a model to be “static” (or “memoryless”) when, at every time instant t , its output is a function of its input at the very same time instant. Conversely, the output of a “dynamic” model also depends on the input values it receives at instants

different from t . In this general sense, we say that it has a “memory” (or, equivalently, a “state”). Constant gains as (2) or (4) are linear static models offering an extremely simple proportional relation between two processes. We propose a dynamic extension of the linear approach just described in the previous section based on the well-known Wiener Filter.

Given two stochastic processes X_i , X_j and a time discrete transfer function $W_{ji}(z)$ (that is the zeta-transform of its impulse response), let us consider the quadratic cost

$$E [(\varepsilon_Q)^2] \quad (7)$$

where

$$\varepsilon_Q \doteq Q(z)(X_j - W_{ji}(z)X_i) \quad (8)$$

being $Q(z)$ an arbitrary stable and causally invertible time-discrete transfer function weighting the error

$$e_{ji} = X_j - W_{ji}(z)X_i. \quad (9)$$

Then, the problem of evaluating the transfer function $\hat{W}(z)$ such that the quadratic cost (7) is minimized is well-known in scientific literature and its solution is referred to as the Wiener filter (see [13]).

Proposition 3 (Wiener filter). *The Wiener filter modeling X_j by X_i is the linear stable filter \hat{W}_{ji} minimizing the filtered quantity (7). Its expression is given by*

$$\hat{W}_{ji}(z) = \frac{\Phi_{X_i X_j}(z)}{\Phi_{X_i}(z)} \quad (10)$$

and it does not depend upon $Q(z)$. Moreover, the minimized cost is equal to

$$\min E [(Q(z)\varepsilon)^2] = \frac{1}{2\pi} \int_{-\pi}^{\pi} |Q(\omega)|^2 (\Phi_{X_j}(\omega) - |\Phi_{X_j X_i}(\omega)|^2 \Phi_{X_i}^{-1}(\omega)) d\omega$$

Proof. See, for example, [13] □

Observe that the stable implementation of the Wiener filter $\hat{W}_{ji}(z)$ is non-causal, in general. That is, its output $\hat{W}_{ji}(z)X_i$ depends on both past and future values of the input process X_i . The Wiener filter, in this formulation, is interesting from an information and modeling point of view, but, of course, we would rather need a causal filter, if we were to make predictions (aim which is beyond the scope of this paper). Since the weighting function $Q(z)$ does not affect the Wiener filter, but only the energy of the filtered error, we choose $Q(z)$ equal to $F_j(z)$, the inverse of the spectral factor of $\Phi_{X_j}(z)$, that is

$$\Phi_{X_j}(z) = F_j^{-1}(z)(F_j^{-1}(z))^* \quad (11)$$

with $F_j(z)$ stable and causally invertible (see [15]). In such a case the minimum cost assumes the value

$$\min E[\varepsilon_{F_j}^2] = \frac{1}{2\pi} \int_{-\pi}^{\pi} \left(1 - \frac{|\Phi_{X_j X_i}(\omega)|^2}{\Phi_{X_i}(\omega)\Phi_{X_j}(\omega)} \right) d\omega. \quad (12)$$

This peculiar choice of $Q(z)$ makes the cost depend explicitly on the coherence function of the two processes

$$C_{X_i X_j}(\omega) \doteq \frac{|\Phi_{X_j X_i}(\omega)|^2}{\Phi_{X_i}(\omega)\Phi_{X_j}(\omega)} \quad (13)$$

which turns to be non negative and symmetric with respect to ω . It is also well-known that the cross-spectral density satisfies the Schwartz inequality. Hence, the coherence function is limited between 0 and 1. The choice $Q(z) = F_j(z)$ can be now understood as motivated by the necessity to achieve an adimensional cost function not depending on the power of the signals as in (12).

The cost obtained by the minimization of the error ε_{F_j} using the Wiener filter as before allows us to define the binary function

$$d(X_i, X_j) \doteq \left[\frac{1}{2\pi} \int_{-\pi}^{\pi} (1 - C_{X_i X_j}(\omega)) d\omega \right]^{1/2}. \quad (14)$$

Proposition 4. *The function $d(\cdot, \cdot)$, as defined in (14) is a metric.*

Proof. See the appendix. \square

The metric (14) can now be used to derive a MST and obtain a hierarchical structure of the processes X_i . Such an approach generalizes the results in [9] to the linear dynamic case. We remark that the choice of a tree to describe the topology of the data is a very reasonable but arbitrary solution. In order to capture influences and similarities among the processes X_j , we intend to propose a more flexible modeling technique to extract topological information from the data. Every X_j can be described as the output of a linear SISO dynamical system, whose input is one of the other $N-1$ processes. Thus, for every time series X_j it is natural to choose the model $\hat{W}_{jm(j)}$ with input $X_{m(j)}$, such that it provides the best description according to (12), dropping the others. The application of this procedure results in a set N interconnected systems, each of them minimizing $\min_i E[(Q_j e_{ji})^2]$. Since the choice of every model $\hat{W}_{jm(j)}$ does not affect the selection of the other ones, the overall cost function

$$\min_{m(\cdot)} \sum_j E[(Q_j e_{jm(j)})^2] \quad (15)$$

turns out to be minimized, as well. The following algorithm performs such a task.

Clusterization Algorithm:

1. initialize the set $A = \emptyset$
2. for every process X_j ($j = 1, \dots, N$)
 - 2a. for every $i = 1, \dots, N, i \neq j$
compute the distance $d_{ij} \doteq d(X_i, X_j)$;
 - 2b. define the set $M(j) \doteq \{k | d_{kj} = \min_i d_{ij}\}$
 - 2c. choose, if possible, $m(j) \in M(j)$ such that $(m(j), j) \notin A$
 - 2d. choose the model
 $X_j = \hat{W}_{jm(j)}(z)X_{m(j)} + e_{jm(j)}$
 - 2e. add the couple $(j, m(j))$ to A .

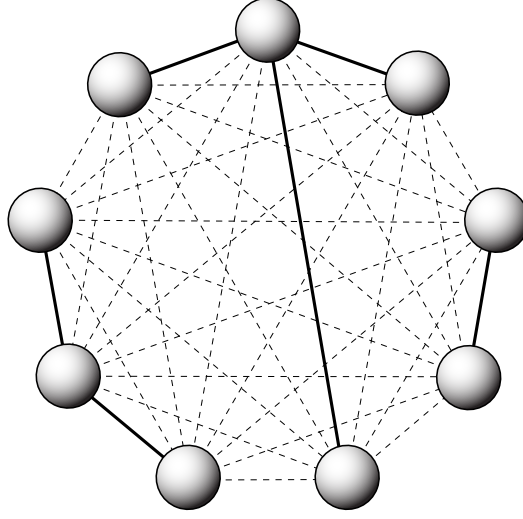


Figure 1. The figure illustrates all the possible connections between two nodes (dashed lines) in a nine-node network. The solid lines depict a forest as it were the result after the application of the algorithm A.

Figure 2. The figure illustrates all the possible connections between two nodes (dashed lines) in a 10 nodes network. The solid lines depict a forest as it were the result after the application of the clusterization algorithm.

The resulting network of processes has an appealing graphical interpretation. Indeed, its topological structure can be seen as a weighed graph where every process X_j is a node, the arc linking X_i to X_j represents the Wiener Filter describing the “output” X_j in terms of the “input” X_i and the weights on the arcs are given by (14). Because of the symmetry property of (14), there is no actual need to consider an oriented graph. Hence, the presence of both the arcs (i, j) and (j, i) boils down into just a single link. Following this interpretation, the algorithm determinates a graph designed to keep, for every node, the incident arc with the least cost (see Figure 1).

Proposition 5. *The graph resulting from the proposed algorithm has the following properties:*

- on every node there is at least an incident arc
- if there is a cycle, then all the arcs of the cycle have the same weight
- there are at least $\lceil N/2 \rceil$ and at most N arcs.

Proof. See the appendix. □

The presence of cycles in the resulting graph is a pathological situation as stressed in the following remark.

Remark 6. *A necessary condition of existence for a cycle is the presence of more than two nodes with common multiple minimum cost arcs. Therefore, a mild sufficient condition in order to avoid cycles in the graph is to assume that every node has a unique minimum cost arc. If the costs of the arcs are obtained by estimation from real data the probability to obtain a cycle is zero almost everywhere (see [16]). Consequently, in such a case the expected topology of the graph is a forest (a graph with no cycles).*

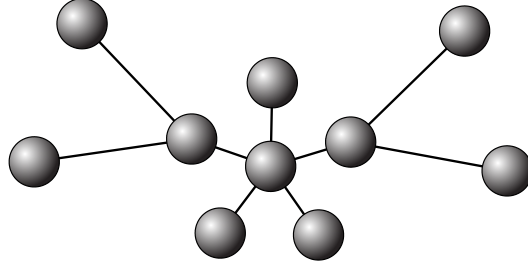


Figure 3. The figure illustrates the topology of the 10 nodes network analyzed in the numerical examples paragraph. Each node represent a process X_j , while the arcs describe the connections among them, according to the linear SISO model (16). For the data generation we have considered only transfer functions of at most the second order. The noises N_j have been assumed to provide half the power of the affected processes. The samples have been collected over 1000 time steps.

Remark 7. *If there are no cycles, the graph resulting from the algorithm is a subgraph of the MST.*

Remark 8. *In general, nothing can be said about the connectivity. Therefore, the modeling procedure depicted by the algorithm provides a clusterization of the original processes X_i which, for every node, minimizes the cost (14) according to the criterion of linear dynamic dependency. It is possible to modify the procedure in order to suitably satisfy other constraints about the graph topology. For instance, if we deal with a connectivity condition the algorithm can be easily replaced by a MST search. Therefore, the approach followed in [9] to obtain topological information from the time series results in a constrained optimization of (15).*

Remark 9. *The modelization we have derived makes use of non causal Wiener filters, thus it can be useful to detect linear dependencies of any sort between the processes X_i .*

Unfortunately, the adoption of non causal filters can not be employed to make predictions.

4. Numerical Example

It is intended to show, by means of numerical examples, the main advantages of the technique described in the previous sections. In particular, we want to evaluate the performance of our procedure when identifying an unknown topology. First, we realized several simulations of 10 randomly generated processes X_j , designed as follows. They have been hierarchiacally structured in a tree topology, where the interconnections were linear, randomly generated, at most second order transfer functions W_{ji} with external noise N_j .

$$X_{ji} = W_{ji}(z)X_i + N_j \quad (16)$$

Since all simulations present strong analogies, we are showing just one of them, whose topology is depicted in Figure 3. Note that the simulated network involves linear dependencies only, so it satisfies the theoretical conditions of the approach

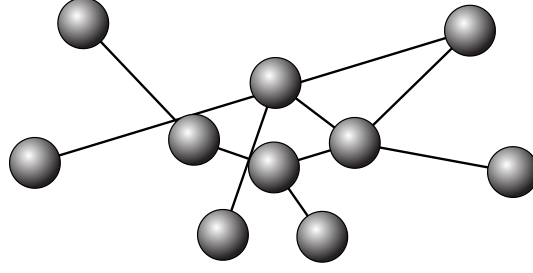


Figure 4. The MST obtained using the correlation-based distance of Table(1). The actual topology has not been correctly identified, though some analogies with the right structure can be observed. The procedure described in [4] reveals strong limitation in capture the nature of the network even when the actual topology is exactly a tree.

based on Wiener filters introduced in the previous sections. On every node X_j (but the root) the deterministic component $W_{ji}(z)X_i$ and the stochastic disturbance are equal in power. A simulation horizon of 1000 steps has been taken into account where the noise components have been generated by pseudo random number algorithms. The incorrelation hypothesis among the disturbances has been numerically checked providing a marginally satisfactory result. Applying the correlation technique described in [4], we found the distance matrix reported in Table 1 and the corresponding MST depicted in Figure 7. We note that the topology is not correctly

	X_1	X_2	X_3	X_4	X_5	X_6	X_7	X_8	X_9	X_{10}
X_1	0	0.9946	1.3763	1.0624	1.1027	1.2393	1.2719	1.3747	0.7306	1.4589
X_2	0.9946	3.3e-8	1.1130	1.0674	0.7723	1.0082	1.2004	1.1269	1.1132	1.4575
X_3	1.3763	1.1130	0	1.1487	1.2217	1.2877	1.1645	0.9965	1.3507	1.4124
X_4	1.0624	1.0674	1.1487	4.2e-8	1.1727	1.1805	0.9296	1.1455	1.1491	1.3433
X_5	1.1027	0.7723	1.2217	1.1727	3.9e-8	1.1491	1.2418	1.2353	1.1898	1.4587
X_6	1.2393	1.0082	1.2877	1.1805	1.1491	4.9e-8	1.2123	1.2984	1.2858	1.3227
X_7	1.2719	1.2004	1.1645	0.9296	1.2418	1.2123	0	1.1815	1.3003	1.3334
X_8	1.3747	1.1269	0.9965	1.1455	1.2353	1.2984	1.1815	0	1.3542	1.4389
X_9	0.7306	1.1132	1.3507	1.1491	1.1898	1.2858	1.3003	1.3542	7.3e-8	1.4450
X_{10}	1.4589	1.4575	1.4124	1.3433	1.4587	1.3227	1.3334	1.4389	1.4450	0

Table 1. Correlation-based distance matrix.

identified by such a procedure, even though similarities can be identified. On the other hand, the application of the clusterization algorithm introduced by us provides the distances of Table 2 with the graph of Figure 5. We stress that the topology

	X_1	X_2	X_3	X_4	X_5	X_6	X_7	X_8	X_9	X_{10}
X_1	0	0.7299	0.6675	0.7351	0.8316	0.8542	0.8297	0.7055	0.6549	0.8298
X_2	0.7299	0	0.8065	0.8353	0.6934	0.7358	0.8786	0.8483	0.8299	0.8717
X_3	0.6675	0.8065	0	0.8216	0.8744	0.8807	0.8750	0.8262	0.7841	0.8821
X_4	0.7351	0.8353	0.8216	0	0.8662	0.8722	0.7404	0.8502	0.8198	0.7039
X_5	0.8316	0.6934	0.8744	0.8662	0	0.8540	0.8919	0.8995	0.8730	0.8846
X_6	0.8542	0.7358	0.8807	0.8722	0.8540	0	0.8934	0.8984	0.8796	0.8944
X_7	0.8297	0.8786	0.8750	0.7404	0.8919	0.8934	0	0.8838	0.8694	0.8346
X_8	0.7055	0.8483	0.8262	0.8502	0.8995	0.8984	0.8838	0	0.8167	0.8908
X_9	0.6549	0.8299	0.7841	0.8198	0.8730	0.8796	0.8694	0.8167	0	0.8715
X_{10}	0.8298	0.8717	0.8821	0.7039	0.8846	0.8944	0.8346	0.8908	0.8715	0

Table 2. Coherence-based distance matrix.

is perfectly reconstructed by the procedure if the connectivity constraint is imposed. Further, we repeated the same procedure with a larger number of processes ($N = 50$). Again, results showed many similarities, so we are presenting just one case with the topology depicted in Figure 6 Analogously, the correlation-based approach provides

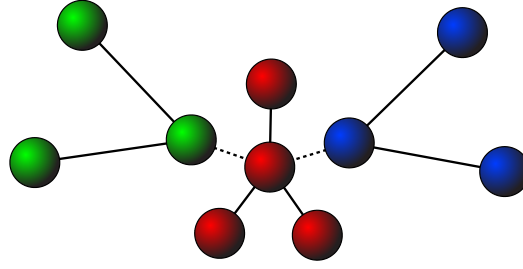


Figure 5. The figure illustrates the MST obtained by using the coherence-based distance (solid+dashed lines). Notably, it is the same of the actual topology. The application of the proposed clustering algorithm provides a forest (solid lines): each cluster is virtually connected to the others by the arcs of the MST, which have not been chosen by the algorithm (dashed lines). The use of different colors (online) highlights the modular structure resulting from the clusterization. The presence of a very high noise-to-signal ratio prevents the algorithm to correctly reconstruct the actual topology, if no connectivity constraint is given.

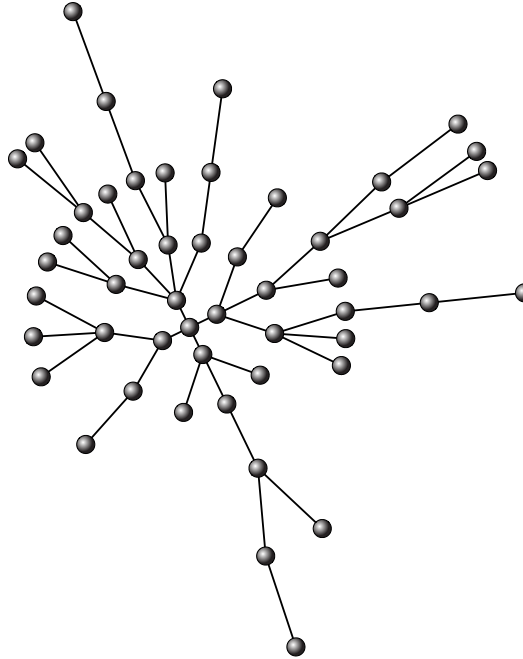


Figure 6. The 50 nodes network of the numerical examples paragraph. The figure provides the actual topology. The example has been designed according to the same assumptions of the network of Figure 6.

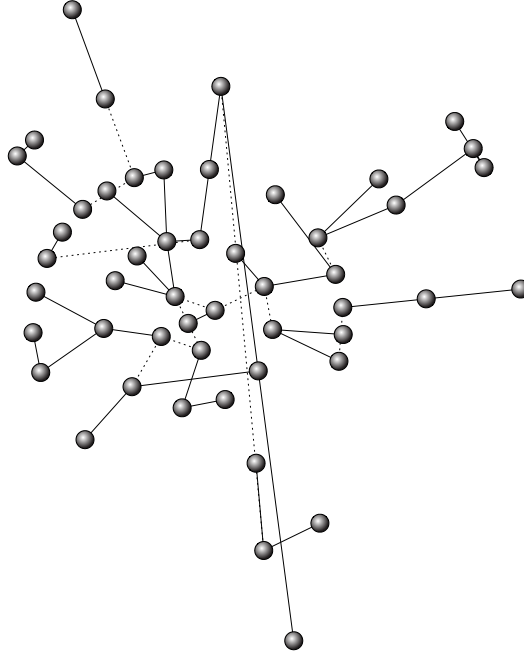


Figure 7. The figure illustrates the MST obtaining by means of the correlation-based distance. Though the original topology is a tree, a quite significant amount of connections have not been correctly reconstructed. A limited number of similarities with the actual network can be observed.

the MST of Figure 7 while the coherence-based algorithm identifies the graph of Figure 8. It is worth noting that our technique detects links actually present in the topology. However the presence of a low signal to noise ratio prevents the complete reconstruction of the original tree topology in the absence of any connectivity constraints. These simple examples highlight a better capability of our technique into capturing relationships and dependencies among time series. In particular, remarkable improvements should be expected in presence of strong dynamical interconnections and significative delays in the actual network.

5. Conclusions

In this paper we have introduced a novel approach to the clusterization problem. In particular, the similarities among the time series of a multivariate data set have been analyzed from the modeling point of view and their interconnections have been interpreted as functional dependencies. Hence, linear SISO transfer functions have been proposed to describe the relations among the processes and the associated modeling errors have been exploited to quantify their similarities. In turn, such a distance introduces a natural way of grouping the time series, since it is very reasonable to place two processes in the same subset, when one provides the best model to explain the other. Notably, the proposed distance can be directly computed exploiting the coherence function, requiring no identification step. Further, our novel approach

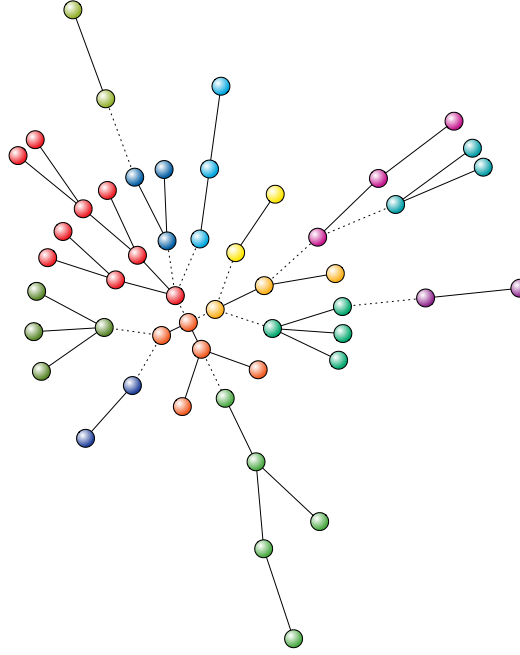


Figure 8. The figure show the MST (solid+dashed lines) obtained by applying the coherence-based distance (16) to the processes produced by the network depicted in Figure 6. Notably, the original structure has been correctly reconstructed. The forest resulting from the application of the clusterization algorithm is also reported (solid lines). The clusters (colors online) result connected by the remaining arc of the MST (dashed lines). The algorithm does not manage to reconstruct exactly one cluster, because of the high noise-to-signal ratio.

has been compared to the clustering technique proposed in [4] and formulated as an extension of the multivariate analysis of [8]. In particular, our coherence-based distance turns out to be the dynamical generalization of the correlation-based metric in [9]. Therefore, it provides an improved capability in capturing the internal topology among the processes, especially when their functional dependencies turns out to be dynamical laws. Some numerical examples have finally been presented to illustrate the expected improvements, due to our distance, and to provide a validation for our clustering algorithm.

6. Appendix

Proof of Proposition 1 . Note that we consider two processes be equivalent also when they are anticorrelated since they are identical from an information point of view. Thus, the only non trivial property to show is the triangle inequality. Consider the

following relations involving the optimal gains $\hat{\alpha}_{31}$, $\hat{\alpha}_{32}$, $\hat{\alpha}_{21}$

$$\begin{aligned} X_3 &= \hat{\alpha}_{31}X_1 + e_{31} \\ X_3 &= \hat{\alpha}_{32}X_2 + e_{32} \\ X_2 &= \hat{\alpha}_{21}X_1 + e_{21} . \end{aligned}$$

Since $\hat{\alpha}_{31}$ is the best constant model, we have that it must perform better than any other constant model (in particular $\hat{\alpha}_{32}\hat{\alpha}_{21}$)

$$R_{X_3} - \frac{R_{X_3X_1}^2}{R_{X_1}} \leq E[(e_{32} + \hat{\alpha}_{32}e_{21})^2] \leq \left(\sqrt{E[e_{32}^2]} + |\hat{\alpha}_{32}|\sqrt{E[e_{21}^2]} \right)^2 .$$

Normalize with respect to R_{X_3} and consider the square root

$$\begin{aligned} \sqrt{1 - \rho_{X_1X_3}^2} &\leq \sqrt{\frac{1}{R_{X_3}} \left(\sqrt{E[e_{32}^2]} + |\hat{\alpha}_{32}|\sqrt{E[e_{21}^2]} \right)^2} \leq \\ &= \sqrt{\frac{E[e_{32}^2]}{R_{X_3}}} + |\rho_{X_2X_3}| \sqrt{\frac{E[e_{21}^2]}{R_{X_2}}} . \end{aligned}$$

Since $|\rho_{X_2X_3}| \leq 1$, we have the assertion. \square

Proof of Proposition 4 The only non trivial property to prove is the triangle inequality. Let $\hat{W}_{ji}(z)$ be the Wiener filter between X_i, X_j computed according to (10) and e_{ji} the relative error. The following relations hold:

$$\begin{aligned} X_3 &= \hat{W}_{31}(z)X_1 + e_{31} \\ X_3 &= \hat{W}_{32}(z)X_2 + e_{32} \\ X_2 &= \hat{W}_{21}(z)X_1 + e_{21} . \end{aligned}$$

Since $\hat{W}_{31}(z)$ is the Wiener filter between the two processes X_1 and X_3 , it performs better at any frequency than any other linear filter, such as $\hat{W}_{32}(z)\hat{W}_{21}(z)$. So we have

$$\begin{aligned} \Phi_{e_{31}}(\omega) &\leq \Phi_{e_{32}}(\omega) + |\hat{W}_{32}(\omega)|^2 \Phi_{e_{21}}(\omega) + \\ &+ \Phi_{e_{32}e_{21}}(\omega) \hat{W}_{32}^*(\omega) + \hat{W}_{32}(\omega) \Phi_{e_{21}e_{32}}(\omega) \leq \\ &\leq (\sqrt{\Phi_{e_{32}}(\omega)} + |\hat{W}_{32}(\omega)|\sqrt{\Phi_{e_{21}}(\omega)})^2 \quad \forall \omega \in \mathbb{R} . \end{aligned}$$

For the sake of simplicity we neglect to explicitly write the argument ω in the following passages. Normalizing with respect to Φ_{X_3} , we find

$$\frac{\Phi_{e_{31}}}{\Phi_{X_3}} \leq \frac{1}{\Phi_{X_3}} (\sqrt{\Phi_{e_{32}}} + |\hat{W}_{32}|\sqrt{\Phi_{e_{21}}})^2$$

and considering the 2-norm properties

$$\left(\int_{-\pi}^{\pi} \frac{\Phi_{e_{31}}}{\Phi_{X_3}} d\omega \right)^{\frac{1}{2}} \leq \left(\int_{-\pi}^{\pi} \frac{\Phi_{e_{32}}}{\Phi_{X_3}} d\omega \right)^{\frac{1}{2}} + \left(\int_{-\pi}^{\pi} \frac{|\Phi_{X_3X_2}|^2 \Phi_{e_{21}}}{\Phi_{X_3} \Phi_{X_2}} d\omega \right)^{\frac{1}{2}}$$

where we have substituted the expression of \hat{W}_{32} . Finally, considering that

$$0 \leq \frac{|\Phi_{X_3 X_2}|^2}{\Phi_{X_3} \Phi_{X_2}} \leq 1,$$

we find

$$d(X_1, X_3) \leq d(X_1, X_2) + d(X_2, X_3).$$

□

Proof of Proposition 5 The proof of the first property is straightforward because for every node the algorithm considers an incident arc. Let us suppose there is a cycle and be k the number of nodes n_1, \dots, n_k and arcs a_1, \dots, a_k of such a cycle. Every arc a_1, \dots, a_k has been chosen at the step 2e when the algorithm was taking into account one of the nodes n_1, \dots, n_k . Conversely, every node n_1, \dots, n_k is also responsible for one of the arcs a_1, \dots, a_k . Indeed, if a node n_i causes the selection of an arc $\hat{a} \notin \{a_1, \dots, a_k\}$, then we are left with the k arcs which cannot all be chosen by $k - 1$ nodes.

Let us consider the node n_1 . Without loss of generality assume that it is responsible for the selection of the arc a_1 with weight d_1 and linking it to the node n_2 . According to the previous results, n_2 can not be responsible for the choice of a_1 . Let a_2 be the arc selected because of n_2 with weight d_2 and connecting it to n_3 . Observe that necessarily $d_2 \leq d_1$. We may repeat this process till the node n_{k-1} . Hence, we obtain that every node n_i is connected to n_{i+1} by the arc a_i whose cost is $d_i \leq d_{i-1}$, for $i = 2, \dots, k - 1$. Finally consider n_k . It must be responsible for a_k which has to connect it to n_1 with cost $d_k \leq d_{k-1}$. Since d_k is incident to n_1 it holds that $d_1 \leq d_k$. Therefore $d_1 \leq d_k \leq d_{k-1} \dots \leq d_2 \leq d_1$ and we have the assertion of the second property.

About the third property, the upper bound N follows from the consideration that every node causes the choice of at most a new arc. In step 2c of the algorithm, it may happen at most $\lfloor N/2 \rfloor$ times that we are forced to pick up an arc which is already in A . So we have at least $N - \lfloor N/2 \rfloor = \lfloor N/2 \rfloor$ arcs □

References

- [1] M. Blatt, S. Wiseman, and E. Domany. Super-paramagnetic clustering of data. *Physical Review Letters*, 76:3251, 1996.
- [2] E. Ravasz, A. L. Somera, D. A. Mongru, Z. N. Oltvai, and A. L. Barabási. Hierarchical organization of modularity in metabolic networks. *Science*, 297:1551, 2002.
- [3] R. G. Palmer, D. L. Stein, E. Abrahams, and P. W. Anderson. Models of hierarchically constrained dynamics for glassy relaxation. *Phys. Rev. Lett.*, 53(10):958–961, Sep 1984.
- [4] R. N. Mantegna. Hierarchical structure in financial markets. *Eur. Phys. J. B*, 11:193–197, 1999.
- [5] K. V. Mardia, J. T. Kent, and J. Bibby. *Multivariate Analysis*. Academic Press, London, UK, 1979.
- [6] M. Anderberg. *Cluster Analysis for Applications*. Academic Press, New York, 1973.

- [7] M. B. Eisen, P. T. Spellman, P. O. Brown, and D. Botstein. Cluster analysis and display of genome-wide expression patterns. *Proc Natl Acad Sci U S A*, 95(25):14863–8, 1998.
- [8] M. Tumminello, C. Coronello, F. Lillo, S. Micciché, and R. N. Mantegna. Spanning trees and bootstrap reliability estimation in correlation-based networks. *Int. J. of Bifurcations & Chaos*, 17:2319–2329, 2007.
- [9] R. N. Mantegna and H. E. Stanley. Scaling behaviour in the dynamics of an economic index. *Nature*, 376:46–49, 1995.
- [10] P. Gopikrishnan, V. Plerou, L. A. N. Amaral, M. Meyer, and H. E. Stanley. Scaling of the distributions of fluctuations of financial market indices. *Phys. Rev. E*, 60:5305–5316, 1999.
- [11] M. J. Naylora, L. C. Roseb, and B. J. Moyle. Topology of foreign exchange markets using hierarchical structure methods. *Physica A*, 382:199–208, 2007.
- [12] Lennart Ljung. *System identification: theory for the user (2nd Ed.)*. Prentice-Hall, Inc., Upper Saddle River, NJ, USA, 1999.
- [13] T. Kailath, A. H. Sayed, and B. Hassibi. *Linear Estimation*. Prentice Hall, Upper Saddle River, New Jersey, 2000.
- [14] Clive W. J. Granger. Investigating causal relations by econometric models and cross-spectral methods. *Econometrica*, 37:424–438, 1969.
- [15] A. H. Sayed and T. Kailath. A survey of spectral factorization methods. *Numerical Linear Algebra with Applications*, 8:467–469, 2001.
- [16] A. N. Shiryaev. *Probability*. Springer-Verlag, New York, 1995.